Hydrothermal recycling of carbon absorbents loaded with emerging wastewater contaminants

Environmental Pollution 316 (2023) 120532

Contents lists available at ScienceDirect

Environmental Pollution

journal homepage: www.elsevier.com/locate/envpol

Hydrothermal recycling of carbon absorbents loaded with emerging wastewater contaminants☆

Christian Wurzer [a,*], Pierre Oesterle [b], Stina Jansson [b], Ondřej Mašek [a]

[a] UK Biochar Research Centre, School of GeoSciences, Crew Building, The King's Buildings, University of Edinburgh, EH9 3FF Edinburgh, UK
[b] Department of Chemistry, Umeå University, SE-901 87 Umeå, Sweden

ARTICLE INFO

Keywords:
Activated carbon
Engineered biochar
Iron doping
Pharmaceuticals
Adsorbent recycling

ABSTRACT

Adsorption using carbon materials is one of the most efficient techniques for removal of emerging contaminants such as pharmaceuticals from wastewater. However, high costs are a major hurdle for their large-scale application in areas currently under economic constraints. While most research focuses on decreasing the adsorbent price by increasing its capacity, treatment costs for exhausted adsorbents and their respective end-of-life scenarios are often neglected. Here, we assessed a novel technique for recycling of exhausted activated biochars based on hydrothermal treatment at temperatures of 160–320 °C. While a treatment temperature of 280 °C was sufficient to fully degrade all 10 evaluated pharmaceuticals in solution, when adsorbed on activated biochars certain compounds were shielded and could not be fully decomposed even at the highest treatment temperature tested. However, the use of engineered biochar doped with Fe-species successfully increased the treatment efficiency, resulting in full degradation of all 10 parent compounds at 320 °C. The proposed recycling technique showed a high carbon retention in biochar with only minor losses, making the treatment a viable candidate for environmentally sound recycling of biochars. Recycled biochars displayed potentially beneficial structural changes ranging from an increased mesoporosity to additional oxygen bearing functional groups, providing synergies for subsequent applications as part of a sequential biochar system.

1. Introduction

The use of carbon materials for the adsorption of emerging contaminants is one of the most efficient means of tertiary wastewater treatment (Rizzo et al., 2019). With their high adsorption capacity, activated carbons are the current benchmark material for a variety of pollutant classes including emerging contaminants such as pharmaceuticals and personal care products (Rout et al., 2021). However, the widespread use of activated carbon is hindered by high costs and consequently mainly limited to developed countries with stringent environmental protection, e.g. Switzerland, Germany or Sweden (Baresel et al., 2019).

Biochar – a class of low-cost carbon adsorbents (Ahmed et al., 2015) – has been extensively researched as an economic and environmental means to enable the expansion of tertiary wastewater treatment to areas currently under economic constraints (Fdez-Sanromán et al., 2020). As the main cost drivers of activated carbons are the production, transportation and regeneration of the adsorbent, biochar requiring lower energy input during production and utilising regionally available biomass waste streams provide a promising alternative (Joseph et al., 2020). However, the overall cost of a remediation effort using a certain adsorbent material is determined not only by the economic cost of purchase or production of the material but also by the amount required for the expected removal outcome, which is in turn determined by the material's adsorption performance. The overall cost can be displayed as the cost of removing a specified mass of contaminant from a given matrix, and treatment costs of exhausted adsorbents (Alhashimi and Aktas, 2017; Patel et al., 2019). Pristine biochars often display unsatisfactory adsorption capacities which add additional handling, storage and treatment costs due to the large amounts of adsorbents required (Krasucka et al., 2021). Common differences in adsorption capacities between pristine biochar and activated carbon can be in the order of magnitudes which often extinguish potential economic and environmental advantages of biochar (Kozyatnyk et al., 2020; Krasucka et al., 2021). Research on engineering biochar therefore often focuses on increasing its adsorption capacity (Duan et al., 2019). While engineered

☆ This paper has been recommended for acceptance by Dr. Jörg Rinklebe.
* Corresponding author.
E-mail address: c.wurzer@ed.ac.uk (C. Wurzer).

https://doi.org/10.1016/j.envpol.2022.120532
Received 13 July 2022; Received in revised form 6 September 2022; Accepted 24 October 2022
Available online 30 October 2022

biochar can achieve excellent adsorption performance (Wang et al., 2020), extensive modification techniques can present trade-offs (Sizmur et al., 2017), such as lower yields (Jang and Kan, 2019), higher production costs (Nguyen et al., 2019), secondary pollution from the production process (Sewu et al., 2020; Wang et al., 2020), or the unsuitability for subsequent soil application (Duan et al., 2019). For extensively modified biochars, the renewable feedstock source might remain as the only advantage of biochar in comparison to fossil based activated carbons while the complexity of the production processes and feedstock requirements increases. A sole focus on adsorption capacity might therefore be of limited value for providing significant economic or environmental improvements for engineered biochars.

Beside the adsorption performance, the treatment of exhausted carbon adsorbents is an often overlooked cost factor (Zanella et al., 2014). Current research on treatment technologies for exhausted carbon adsorbents is almost entirely focused on regeneration methods, as these enable the reuse of the material for a limited number of cycles and therefore directly lower wastewater treatment costs (Zanella et al., 2014). While a variety of regeneration method exists, even the most common thermal regeneration induces significant costs (Dutta et al., 2019), rendering regeneration often inefficient and resulting in the incineration of exhausted adsorbents (Salvador et al., 2015). For biochar, efficient regeneration will be even more difficult to achieve as the costs of treating high volumes of biochar will be prohibitive. Although mostly neglected (Thompson et al., 2016), existing end-of-life scenarios for exhausted biochar adsorbents are thus often limited to landfilling or incineration. This lack of research on alternative treatment steps might obstruct the environmental and economic potential of biochar as a sustainable low-cost adsorbent through negligence of its purpose as a negative emission technology. Hagemann et al. (2018) defined the differentiating parameter between biochar and activated carbon as the purpose of long-term carbon sequestration for the former. Therefore, an efficient use of biochar will require novel treatment techniques targeting biochar's original aims. As stated by Wurzer et al. (2019) recycling without regeneration can present such an alternative scenario for low-cost adsorbents by enabling a continued use of the recycled material in subsequent applications. Recycling focused on decontamination will not be restrained by the need to restore the original adsorbent properties, instead concentrates on degrading the contaminants. Recycled biochar can then be utilised in subsequent applications requiring different material characteristics to provide additional economic revenues while retaining its carbon sequestration potential.

Hydrothermal treatments (HT) utilise the change in solvothermal properties of water under elevated temperature and pressure and might be suitable for such novel recycling treatments. Due to the use of water as the reaction medium, HT have the potential to present advantages in terms of energy consumption and operational procedures in comparison to common thermal regeneration methods which rely on additional drying steps and high operating temperatures (Salvador and Jiménez, 1996). Hydrothermal carbonisation (HTC) and liquefaction (HTL) are differentiated based on the operating temperature of approximately 160–250 °C (HTC) and 250–400 °C (HTL), as well as their main product fraction, i.e. solid or liquid (Huang and Yuan, 2016). While generally directed at the synthesis of solid carbon, HTC is also known to gradually decompose pharmaceuticals (Svahn and Björklund, 2015). The presence of biomass can hereby act as a catalyst for the decomposition of the contaminants (Weiner et al., 2013). However, while most research analysed the fate of pharmaceuticals during biomass conversion (vom Eyser et al., 2015), only a few studies exist on hydrothermal carbonisation of contaminants adsorbed on activated carbon (Sühnholz et al., 2018; Weiner et al., 2017). To our knowledge, the use of hydrothermal treatments for exhausted biochar or activated biochar has not been tested before. Sühnholz et al. (2018) studied hydrothermal regeneration of activated carbon loaded with organic micropollutants at temperatures between 200 and 240 °C, displaying degradation of a variety of micropollutants. However, no observations indicating full conversion of micropollutants such as caffeine, ibuprofen or triclosan were made, rendering HTC conditions insufficient for complete decontamination of loaded adsorbents. In comparison, HTL operated at temperatures between 300 and 320 °C was found to fully degrade pharmaceuticals and pesticides in raw sewage sludge (Silva Thomsen et al., 2020) and led to a significant reduction in TOC content of treated pharmaceutical wastewater (Thakur et al., 2019). However, no studies on the use of HTL conditions for the degradation of pharmaceuticals adsorbed on carbon adsorbents exist today.

Beside the dominating influence of treatment temperature on the stability of pharmaceuticals (Svahn and Björklund, 2015), several transition metals are known to catalytically enhance the decomposition of organic matter, e.g. Fe-species under HTC conditions (Saadattalab et al., 2020), and Cu-species in HTL (Falamarzian et al., 2014). Fe-species are also well known catalysts in biochar production to increase the production efficiency (Collard et al., 2012; Xia et al., 2019), to add magnetic properties to biochar (Lyu et al., 2020; Yi et al., 2019), to enhance the adsorption of pharmaceuticals (Rocha et al., 2020; Wurzer and Mašek, 2021), and to possess catalytic degradation potential (Faheem et al., 2020). Due to the non-toxicity and availability of Fe, the use of doped carbon adsorbents might present multiple advantages for the use in hydrothermal treatment of exhausted adsorbents. Furthermore, metal-doped carbon adsorbents are unsuitable for common thermal regeneration due to increased reactivity of the introduced metals with common oxidising agents (i.e. CO_2, steam), resulting in excessive burn-offs (Duan et al., 2012; Lambert et al., 2002). Therefore, hydrothermal recycling might provide a suitable carbon-efficient alternative for engineered biochar.

In this study, the use of hydrothermal treatments for the recycling of exhausted activated biochars was tested for the first time to evaluate the suitability for biochars of varying elemental composition and structural stability. We used two activated biochars made from softwood and wheat straw pellets, and one commercial activated carbon as a reference material. Additionally, three magnetic activated biochar composites produced from the same feedstocks were included to examine the effect of Fe-doping on the treatment efficiency. The carbon adsorbents were first loaded with a mixture of 10 pharmaceuticals covering a wide range of compound classes. The exhausted adsorbents were then hydrothermally treated over a temperature range of 160–320 °C. After adsorption and HT, the process water and adsorbents were analysed for the remains of the pharmaceutical parent substances. The main aim of this study was the evaluation of changes in the physicochemical properties of the adsorbents before and after the HT at 320 °C as the impact of hydrothermal recycling treatments on activated biochars was previously untested and represent crucial information for the development of sustainable recycling methods for exhausted activated biochar.

2. Materials and methods

2.1. Adsorbents

In this study, a set of five activated biochars previously described in detail in Wurzer and Mašek (2021), and one commercial activated carbon (Aquasorb 2000; Jacobi) were used as adsorbent materials. Briefly, activated biochars were made from softwood pellets (SWP) and wheat straw pellets (WSP) and three magnetic activated biochar composites were produced by mixing the same feedstocks with ochre – an iron rich mining waste – prior to pyrolysis. Pyrolysis was conducted at a highest treatment temperature of 550 °C under N_2 atmosphere, and subsequent activation was conducted under a constant stream of CO_2 at 800 °C. The activated carbon (AquaSorb 5000) represents a commercial reference material for wastewater treatment. All carbon samples were washed in deionised water (DI), dried at 105 °C and sieved to a particle size of 0.125–0.5 mm to avoid a particle size effect as described by Kårelid et al. (2017). Samples were labelled according to the feedstock source followed by the mass of added ochre, i.e. SWP5 denotes softwood pellets

with an addition of 5 wt% (d.b.) ochre prior to pyrolysis.

2.2. Adsorbent characterisation

Carbon adsorbents were characterised before and after HT at 320 °C for C,H,N,S content (ultimate analysis, O by difference), structural stability (TGA - thermogravimetric analysis), textural properties (N_2 physisorption), crystallographic structure (X-ray diffraction), and magnetic susceptibility (MS) as previously described in detail in Wurzer and Mašek (2021). Additionally, surface functionality was evaluated by Fourier-transform infrared spectroscopy (ATR-FTIR) with a 4 cm^{-1} resolution and 32 scans per spectrum between 4000 and 400 cm^{-1}. Solid yields after the hydrothermal treatment were determined in triplicates using a larger sample size of 100 mg of adsorbent and calculated as the difference of the dried (105 °C, overnight) adsorbent before and after HT. Changes in adsorbent properties before and after HT were tested for significance using a two-sample F-test and subsequent two-sample *t*-test ($p < 0.05$; OriginPro).

2.3. Pharmaceuticals and chemicals

The selection of pharmaceuticals was based on Oesterle et al. (2020), representing compounds commonly found in treated wastewater in the European Union and covers a wide range of compound classes (Lindberg et al., 2014; Loos et al., 2013). Two of the compounds, caffeine and fluconazole, also serve as wastewater indicator substances (Yi et al., 2019). The set of compounds covers a wide range of log K_{OW}-values: −0.07 - Caffeine (CAF); 0.5 - Fluconazole (FLU); 0.7 - Trimethoprim (TRI); 2.25 - Carbamazepine (CAR); 2.36 - Hydroxyzine hydrochloride (HYD); 3.01 - Tramadol (TRA); 3.34 - Oxazepam (OXA); 3.95 - Flecainide (FLE); 4.95 – Amitriptyline (AMI); 6.26 – Clotrimazole (CLO). More detailed information about the pharmaceuticals can be found in Table S1. For the adsorption experiments, a multicompound stock solution of 10 pharmaceuticals (analytical grade) was prepared with individual concentrations of 2 mg L^{-1} (CLO and FLE) and 4 mg L^{-1} (AMI, CAF, CAR, FLU, HYD, OXA, TRA, TRI) dissolved in DI water, and 5 wt% methanol (HPLC grade, Fisher Chemical). Dichloromethane (highly pure >99%), methanol and formic acid (FA, 98–100% purity) were used for the extraction of the pharmaceuticals from the carbon samples, following the method described in detail by Oesterle et al. (2020).

2.4. Adsorption and hydrothermal treatment

Adsorption and hydrothermal treatment were performed in standard borosilicate test tubes (Fisher Scientific, UK) as reaction vessels to avoid the risk of potential catalytic effects of steel liners (De Souza et al., 2014). Adsorption tests were conducted by mixing 30 mg (d.b.) of adsorbent with 7 ml of pharmaceutical stock solution within the reaction vessel, corresponding to a contaminant loading of 8 mg g^{-1} of adsorbent and a filling ratio of 60 vol% of the reaction vessel. The vessel was flushed with N_2 to remove residual air before the glass tube was flame sealed, vortexed for 30 s and placed on an overhead shaker for 24 h at ambient temperature to achieve full (>99%) adsorption. The maximum concentration to achieve full adsorption by all adsorbents was tested beforehand. The sealed reaction vessels were then placed into stainless steel reactors (SS-16-HLN-3, Swagelok). The reactors were filled with DI water to approximately 60 vol% and N_2 to counterpressure the inserted sealed glass tubes during the hydrothermal treatment and to avoid bursting under increasing pressure. The sealed reactors were heated in a muffle furnace to the target temperatures between 160 and 320 °C for 4 h with a heating rate of 8 °C min^{-1}. Once cooled, the liquid phase was sampled through 0.45 μm nitrocellulose syringe filters. The char samples were transferred to falcon tubes by flushing with DI water, centrifuged at 4700 rpm for 10 min before the supernatant was removed manually. Control runs with DI water were conducted for all temperatures and adsorbents. Additional blanks with pharmaceutical solution but without carbon adsorbents were conducted to evaluate the influence of prior adsorption to carbon on the degradation of pharmaceuticals in HT conditions.

2.5. Extraction and LC-MS/MS

Extraction of the remaining pharmaceuticals from the adsorbents after HT was done according to Oesterle et al. (2020). Briefly, 10 ml of a stock solution with a ratio of 10:10:1 dichloromethane: methanol: formic acid was mixed with the adsorbent (30 mg), vortexed and sonicated for 20 min. The samples were centrifuged at 4700 rpm for 10 min, the supernatant collected, and a second similar extraction cycle was conducted. The combined supernatants were dried under a stream of N_2, dissolved in 10 ml DI water and filtered through 0.45 μm nitrocellulose syringe filters. 20 μl of internal standard containing approximately 50 ng of the relevant deuterated pharmaceuticals was added before the samples were stored at 4 °C for subsequent liquid chromatography tandem mass spectrometry (LC-MS/MS) using a TSQ Quantum Ultra EMR triple quadrupole mass spectrometer (Thermo Fisher Scientific, San Jose, CA, USA). Targeted LC-MS/MS analysis was performed using online solid phase extraction as described in detail in Lindberg et al. (2014). The supernatant was similarly analysed for remaining pharmaceuticals. Recovery rates were calculated by subtracting the extractable pharmaceutical concentration after the adsorption phase from the initial concentration of the stock solution (Table S3). All experiments and analyses were done in triplicates.

3. Results and discussion

3.1. Degradation of pharmaceuticals in hydrothermal conditions

Hydrothermal treatment of the multi-compound stock solution induced complete conversion of all pharmaceutical parent compounds at the highest treatment temperature of 320 °C (Fig. 1).

Clotrimazole was the least stable compound under HT conditions, displaying no detectable concentration already at the lowest treatment temperature of 160 °C, likely due to rapid thermal hydrolysis in acidic media (Abdel-Moety et al., 2002; OSPAR Commission, 2005). Similarly, oxazepam is prone to degradation in acidic medium under elevated temperatures (>200 °C) (Frigerio et al., 1973), which explains the increased decomposition at lower temperatures compared to the other evaluated contaminants (Fig. 1). Acidic conditions during hydrothermal treatment even in the absence of acidic additives can occur due to the ability of subcritical water to act as an acid or base catalyst or from degradation products of the organic feedstock material during hydrothermal conversion (Akiya and Savage, 2002). The concentrations of the remaining parent compounds decreased to more than 70% of their

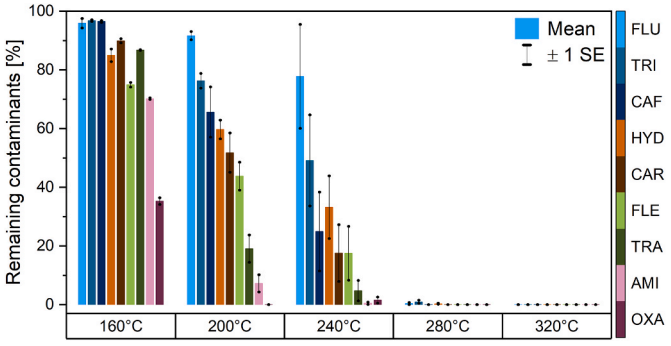

Fig. 1. Degradation of pharmaceuticals in multi-component solution under hydrothermal conditions between 160 and 320 °C. Remaining contaminants after hydrothermal treatment in % of initial concentration. Mean of triplicates. Error bars represent ±1 Standard Error (SE). Results for Clotrimazole were below the detection limit for all temperatures and therefore not shown.

initial concentrations at 160 °C with the highest stability for fluconazole > trimethoprim > caffeine > hydroxyzine. These four pharmaceuticals were found at concentrations higher than 25% at a treatment temperature of 240 °C. A significant step in the degradation was observed between 240 and 280 °C, with almost complete degradation (<1% remaining) at 280 °C for all evaluated contaminants. At 320 °C, none of the parent compounds could be detected. Only a limited number of studies have assessed the degradation of pharmaceuticals under hydrothermal conditions, and even fewer have examined the same compounds of interest. Svahn and Björklund (2015) observed an increase in hydrothermal degradation of several antibiotics and caffeine between 200 and 250 °C, comparable to the reduction in concentration between 240 and 280 °C in this study. The Svahn and Björklund study found caffeine to display a high HT stability of >95% at 250 °C, comparable to results by Sühnholz et al. (2018), but significantly higher than results obtained in this study (25%). For trimethoprim, Taboada-Santos et al. (2019) observed a higher degradation by thermal hydrolysis at 170 °C, while results by Svahn and Björklund (2015) were comparable to this study (59% vs. 100% and 97%). The observed differences between studies might be explained by differences in the composition of the multicompound mixtures, different retention times at the highest treatment temperatures ranging from a few minutes to hours, and non-standardised reactor configurations.

Interestingly, we observed a correlation between log K_{OW} values of the individual contaminants and the degradation efficiency for all analytes except clotrimazole and oxazepam (Figure S2), with lower degradation for highly polar substances (i.e. substances with low log K_{OW}). However, this was not the case in the above mentioned studies, which highlights the need for further research into the degradation mechanisms of pharmaceuticals under hydrothermal conditions.

3.2. The effect of prior adsorption on contaminant degradation

Degradation of contaminants adsorbed to activated softwood biochar (SWP) in relation to the HT temperature can be seen in Fig. 2, with similar general trends for all evaluated adsorbents (Table S4).

Prior adsorption to carbon adsorbents showed increased pharmaceutical degradation at lower temperatures up to 240 °C, in comparison to the treated stock solution, similar to results obtained by Sühnholz et al. (2018). Six out of 10 pharmaceuticals were completely converted at 160 °C, the lowest treatment temperature evaluated, while trimethoprim and carbamazepine were fully degraded at 240 °C. Contrastingly, caffeine and fluconazole showed comparable conversion trends only up to 240 °C between scenarios with and without the presence of adsorbents. A further increase in temperature did not lead to complete degradation of the contaminants. Noteworthy, for all adsorbents and temperatures, most of the non-degraded pharmaceuticals (>99.5%) were observed in the extracts of the adsorbents rather than in the HT aqueous phase (Table S4).

Detectable contaminant concentrations of caffeine and fluconazole even at the highest treatment temperature of 320 °C indicate a protective effect of adsorption (Fig. 3). Pham et al. (2013) and Weiner et al. (2013) described similar results for the hydrothermal conversion of pharmaceuticals in the presence of biomass. Pham et al. (2013) explained the reduced degradation by the low water solubility of the target compounds and a partitioning favouring the adsorption to the solid adsorbent which effectively reduced its degradation. However, the low K_{OW} values of caffeine (−0.07) and fluconazole (0.5) indicate that the observed protective effect is related to the adsorption strength rather than partitioning. If caffeine and fluconazole were desorbed during the hydrothermal treatment, degradation would be expected, and the observed concentrations in the extractions at a treatment temperature of 280 °C can therefore be interpreted as the result of strongly adsorbed compounds. Sato et al. (2018) observed a similar influence of caffeine binding in green coffee beans on its HT extraction efficiency. Strongly adsorbed caffeine on biochars and magnetic biochars, resistant to desorption was also observed by Liyanage et al. (2020).

If the protective effect of prior adsorption is dependent on the desorption rate, it will be determined by the chemical and structural characteristics of the adsorbents. In this study, only small differences between biochars based on their feedstock source could be observed. Activated softwood biochars showed slightly higher degradation efficiency for caffeine (e.g. 15.5% vs. 25.6% remaining caffeine for SWP and WSP respectively) while wheat straw biochars showed increased fluconazole degradation (e.g. 31.9% (SWP) vs. 23.6% (WSP)). A comparison between Fe-doped and undoped samples revealed more pronounced differences with two contrasting trends depending on the HT temperature. At low temperatures of 160 °C and 200 °C, undoped samples showed a lower contaminant retention than doped samples for caffeine

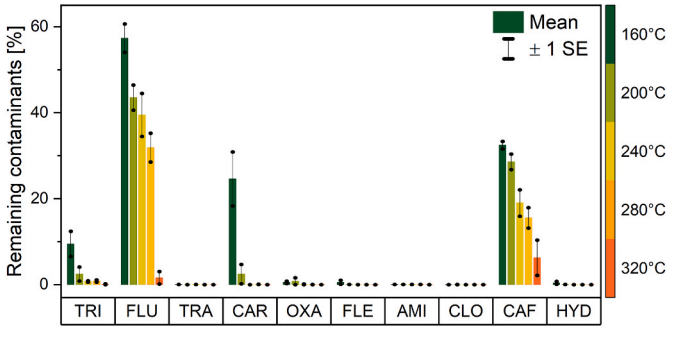

Fig. 2. Degradation of contaminants adsorbed on activated softwood biochar (SWP) with increasing hydrothermal treatment temperature. Mean of triplicates adjusted for experimental recovery rates (Table S3). Error bars represent ±1 Standard Error (SE).

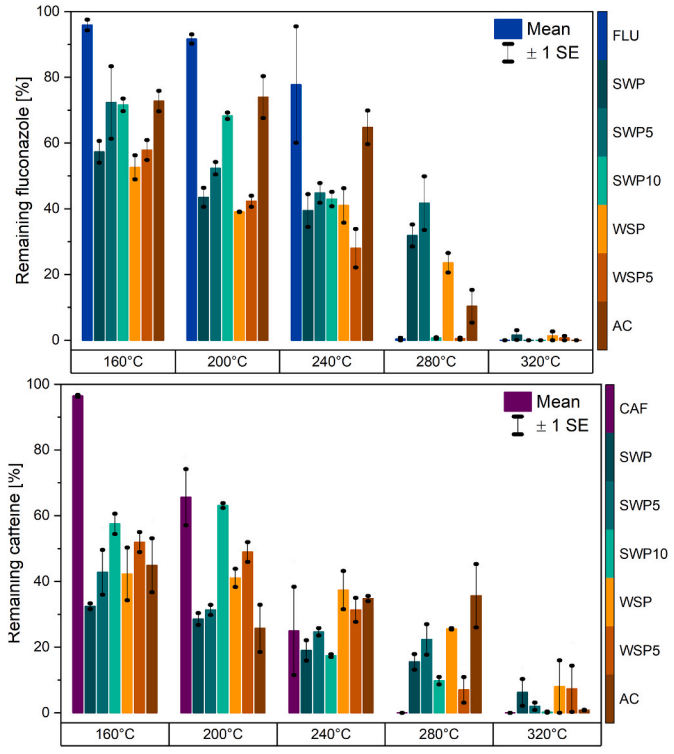

Fig. 3. Remaining fluconazole (FLU; top) and caffeine (CAF; bottom) concentrations (in % of initial concentration) after hydrothermal treatment of all adsorbents (adjusted for recovery rate – Table S3) and stock solution without adsorbent. Mean of triplicates. Error bars represent ±1 standard error (SE). SWP – softwood biochar, SWP5 – softwood biochar doped with 5% ochre, WSP – wheat straw biochar, AC – activated carbon.

(SWP at 160 °C and 200 °C: 32% and 29%; SWP10: 58 and 63%) and fluconazole (SWP: 57% and 44%; SWP10: 72% and 68%). An opposing trend was observed at temperatures from 240 to 320 °C. Here, Fe-doping increased the degradation, indicating a catalytic effect of Fe on the degradation of the pharmaceuticals or differences in the adsorption mechanism to Fe-doped biochars. For caffeine, this resulted in undetectable concentrations at 320 °C for SWP10. For fluconazole, all but two ochre-amended biochars (SWP10 and WSP 5) showed notable protection of the pharmaceutical parent compound from degradation at 280 °C, with more than 24% of the initial concentration remaining in contrast to 0.38% in the absence of an adsorbent. Contrastingly, SWP10 (0.4%) and WSP5 (0.53%) showed similar trace levels of the parent compound as the raw pharmaceutical solution. One possible explanation for these different trends at lower temperatures (160–240 °C) and higher temperatures (>240 °C) might be found in Dittmann et al. (2020). Within their study, adsorption of carbamazepine on activated carbons at low contaminant loadings resulted in preferential adsorption to high-energy adsorption sites, e.g. graphite-like crystallites within the pore structure of activated carbon or heteroatoms within the carbon skeleton. These high-energy adsorption sites proved to be responsible for incomplete desorption and decomposition even at temperatures above the decomposition temperature of pure carbamazepine. In a previous study (Wurzer and Mašek, 2021), the adsorption capacity of the same Fe-doped biochars increased for caffeine by 68% (SWP10) and 193% (WSP5) in contrast to unamended samples (i.e. SWP and WSP). For fluconazole, an increase of 98% (SWP10) and 251% (WSP5) was observed. At low contaminant loadings significantly increased adsorption of caffeine and fluconazole was observed, indicating the presence of similar high-energy adsorption sites, i.e. graphite-like crystallites, in the doped samples (Cai and Larese-Casanova, 2014). This would explain the higher retention of caffeine and fluconazole of Fe-doped samples at low temperatures (i.e. 160 °C and 200 °C) as a result of strong adsorption to defective carbon structures in doped biochar exceeding the desorption energy at low temperatures in comparison to unamended samples. At 240 °C, Fe-doped samples were comparable to unamended samples (e.g. for fluconazole 39.5% vs. 43%; SWP and SWP10), while at 280 °C Fe-doping might catalyse the desorption or degradation of caffeine and fluconazole with a larger effect seen for fluconazole (e.g. 39.1% vs. 0.7%; SWP and SWP10). While catalytic activity of Fe-species are well documented for HTC and HTL (Sun et al., 2010), no studies exist on the effects of Fe-species on the desorption efficiency in subcritical water. Interestingly, the remaining concentrations of caffeine and fluconazole on activated carbon remained relatively constant between 160-240 °C and 160–280 °C, respectively. We hypothesize that strongly bound compounds were seemingly unaffected until a certain temperature was reached at which desorption was initiated, which might in turn indicate a higher homogeneity of occupied adsorption sites on activated carbon than on the assessed biochars.

3.3. Recycled adsorbent properties

Hydrothermal treatment at 320 °C showed minimal solid losses for softwood biochars and activated carbon ranging from 3 to 3.6 wt% (d.b.), with slightly higher losses for wheat straw biochars of 5.4 and 6.5 wt% (d.b.) (Table 1). Solid losses of approximately 5% are similar to supercritical regeneration of activated carbon (3.7–5.1% (Salvador et al., 2013);).

Differences between the feedstocks might be due to loss of water-soluble species such as K, P or Ca as observed in HT of raw biomass (Smith et al., 2016). Degradation products of the pharmaceuticals might also be re-adsorbed to the carbon matrix, however, the total mass change would be minimal as the pharmaceuticals represent less than 1 wt% (d.b.) of the total mass. The high solid yields (>93%) therefore indicate a good stability of carbon adsorbents under harsh hydrothermal conditions at 320 °C and are higher than typical yields in thermal regeneration of 70–90% (Duan et al., 2012; Kozyatnyk et al., 2020).

Ultimate analysis confirmed only moderate changes after HT, with increasing carbon contents for biochars containing a higher initial ash content, resulting in carbon yields ranging from 93.5 to 103.7%. Slightly elevated carbon yields over 100% might be due to the use of filter paper for the yield determination (Whatman Nr.1), with adsorption of dissolved materials from the HTC liquid phase onto the cellulose filter not being included in the subsequent biochar characterisation. The minor carbon losses during the recycling treatment present significant environmental benefits regarding the carbon sequestration potential of the recycled adsorbents. A clear distinction to thermal regeneration can be

Table 1
Physicochemical properties of adsorbents before (bHTC) and after (aHTC) hydrothermal treatment at 320 °C. * indicates significant ($p < 0.05$) difference between bHTC and aHTC. (VM- Volatile Matter, FC – Fixed Carbon, MS – Magnetic Susceptibility, SSA – Specific surface area, Pore size – average pore width, micro PV – micropore volume, meso PV – mesopore volume, total PV – total pore volume).

	Unit	Sample																		
		SWP			SWP 5			SWP 10			WSP			WSP 5			AC			
		bHTC	aHTC		bHTC	aHTC		bHTC	aHTC		bHTC	aHTC		bHTC	aHTC		bHTC	aHTC		
Proximate Analysis																				
VM	wt.%, d.b.	6.7	8.0	*	11.5	14.3	*	15.9	17.3		8.1	7.8		13.0	11.6		2.6	2.1		
FC	wt.%, d.b.	91.4	88.8	*	80.0	75.5	*	67.0	67.3		70.6	76.3	*	55.2	62.6	*	80.4	82.2		
Ash	wt.%, d.b.	1.9	3.1		8.5	10.3		17.1	15.4		21.3	15.9	*	31.8	25.9	*	17.0	15.7		
Ultimate analysis																				
C	wt.%, d.b.	85.68	84.50		70.86	69.97		68.79	72.30		64.06	70.24	*	62.37	68.85	*	76.15	73.90	*	
H	wt.%, d.b.	0.74	1.11	*	0.80	0.79		0.79	0.74	*	0.86	0.88		0.77	0.97	*	0.46	0.67	*	
N	wt.%, d.b.	0.17	0.16		0.14	0.29	*	0.19	0.25	*	0.93	1.04	*	0.77	0.83	*	0.24	0.28	*	
S	wt.%, d.b.	0.08	0.00	*	0.12	0.12		0.11	0.08	*	0.10	0.03	*	0.21	0.15	*	0.86	0.12	*	
O	wt.%, d.b.	11.43	11.10		19.58	18.56		13.02	11.24		12.75	11.92		4.08	3.35		5.29	9.30		
H/C	mol/mol	0.10	0.16	*	0.13	0.13		0.14	0.12	*	0.16	0.15	*	0.15	0.17	*	0.07	0.11	*	
O/C	mol/mol	0.10	0.10		0.21	0.20		0.14	0.12		0.15	0.13	*	0.05	0.04		0.05	0.09	*	
Magnetic S.																				
	10^6 m^3 kg^{-1}	86	306	*	26672	34342	*	47722	50157	*	1	153	*	25450	27105	*	201	245		
XRD			GO		M	M		M	M, GO					M	M, GO					
N_2 physisorption																				
SSA	m^2 g^{-1}	624	432	*	660	365	*	730	595		620	582		506	512		982	853		
Pore size	nm	1.95	2.184		2.018	3.049	*	3.21	3.549	*	1.927	2.678	*	2.128	2.581		2.23	2.081		
micro PV	cm^3 g^{-1}	0.2	0.134	*	0.22	0.117	*	0.185	0.146		0.211	0.152		0.167	0.12		0.547	0.274		
meso PV	cm^3 g^{-1}	0.063	0.076		0.071	0.147		0.221	0.303		0.054	0.152		0.07	0.12		0.24	0.183		
total PV	cm^3 g^{-1}	0.29	0.21	*	0.329	0.264		0.584	0.449		0.295	0.333	*	0.264	0.281	*	0.625	0.457		
HT yield	wt.%, d.b.		97.01			96.36			96.8			94.61			93.54			96.39		

found in the high carbon yield of HT of at least 93%, while mass loss during thermal regeneration can be mostly attributed to the loss of carbon species.

A comparison of volatile matter (VM) and fixed carbon (FC) content of the loaded and hydrothermally treated adsorbents further confirmed the stability of the carbon matrix. While VM for all samples decreased slightly after HT, only SWP10 showed a statistically significant reduction from 15.9 to 13.4%. The fixed carbon content increased for samples with reduced ash content after HT (SWP10, WSP, WSP5), indicating leaching of ash rather than an increased stability of the adsorbent matrix. High ash content samples such as WSP (21.3%) and WSP5 (31.8%) showed the largest reduction of ash content under HT conditions (−5.4% and −5.9%, respectively). A comparison between ochre-amended samples with their pure counterparts indicated that the decrease in ash of WSP biochars was related to the mineral phase of the feedstock itself rather than the ochre addition. Similar losses observed for WSP and WSP5 in combination with no significant reduction of ash content recorded for SWP10 (−1.7%, $p > 0.05$) and even increased ash content for SWP5 (+1.8%, $p > 0.05$) means that no trend could be discerned for the ochre-amended samples. The increasing ash content of SWP and SWP5 can also explain their slightly lowered FC content (−2.6% and −4.5%, $p < 0.05$).

Larger decreases in the ash content of wheat straw biochars will also be influenced by the ash composition. Hydrothermal carbonisation is known to release minerals from the feedstock into the liquid phase, which is further enhanced under hydrothermal liquefaction conditions. Wheat straw biochar contain higher contents of potentially water-soluble species such as Ca, Mg and K (Tab.S7). While all biochars were washed in DI water prior to the adsorption experiments, solvent properties of water at subcritical conditions were vastly increased and might have resulted in additional leaching during HT. It is important to note that the magnetic susceptibility was enhanced for all ochre-amended biochars after hydrothermal treatment (Table 1). This confirms the stability of magnetite/maghemite species present in the biochar composite samples, which was further backed by XRD analysis, and highlights the loss of water-soluble species as the main reason for the decreased ash contents. Hydrothermally treated Fe-doped biochars showed XRD peak signals at 29.95°, 35.25°, 42.9°, 56.9° and 62.4°, confirming the continuous presence of magnetite (Fe_3O_4) or maghemite (γ-Fe_2O_3) (Dastgheib et al., 2014). A comparison of XRD spectra from biochars before and after HT revealed several other changes, with increasing relative peak intensity at 15–30°, representing amorphous carbon and decreasing intensity at 40–50° for graphitic carbon structures. Noteworthy, new peaks emerged at 12° which might indicate the presence of graphene oxide, especially in samples SWP, SWP10, and WSP5. A comparison of XRD patterns of SWP10 before and after HT highlights the appearing peak at 12° which could indicate chemical oxidation of graphitic structures (Fig. 4).

The surface functionality of the treated adsorbents was only marginally influenced by HT. Generally, all biochar samples displayed increasingly similar spectra after HT, i.e. displaying a homogenising effect on the surface of ochre-amended and unamended samples. However, as confirmed by XRD and MS, a peak at 590 cm^{-1} representing Fe_3O_4 vibration in magnetic biochars was largely unaffected, further confirming the stability of magnetite/maghemite during the HT (Ma et al., 2020). All biochars showed a peak shift from 1100 cm^{-1} (C–O–C) to 1025 cm^{-1}, representing C–O vibration, which was significantly more pronounced after HT for SWP5 and SWP10 (Liu et al., 2015; Uchimiya et al., 2011b). Carboxyl peaks at 1740 cm^{-1} were unaffected by HT while C═O intensity (1550-1600 cm^{-1}) increased, especially for SWP (Lou et al., 2016). The creation of additional C–O and C═O bonds might indicate catalytic activity of Fe during HT. While unamended SWP displayed only a significant intensity increase for C═O, SWP5 and SWP10 showed additional high intensity peaks for C–O, pointing towards a higher reactivity of Fe to HT induced oxidation. A decrease in peak intensity for all biochars around 875 cm^{-1} and 1450 cm^{-1} indicates the loss of C═H groups after HT (Jung and Kim, 2014).

Significant changes of HT on biochars can also be noticed for the textural parameters, i.e. SSA, micropore volume, total pore volume, and average pore size. Surface area of all biochars decreased after HT, with larger decreases for softwood biochars than wheat straw biochars (SWP: −30.7%/−192 m^2; WSP: −6.1%/−38 m^2). Contrastingly, Sühnholz et al. (2018) found the SSA of commercial activated carbon to be stable at a temperature of 240 °C, indicating an effect of the harsher treatment conditions (320 °C) applied in this study. The observed decrease in SSA is also reflected in the pore volumes and can be solely related to the micropore region of the biochars while the mesopore region (SSA and pore volume) increased for all samples (Table 1). Mustafa et al. (2021) observed the re-adsorption of transformation products after regeneration to significantly decrease the micropore surface area of activated carbons, which might also be the case during HT. Additionally, pore size distributions revealed a swelling of mesopores (Fig. 4 and S3) and due to the parallel closure of narrow micropores the average pore diameter increased for all biochars into mesopore dominated (>2 nm). The increase in mesopore volume could be related to the leaching of minerals as mentioned before and also reported by Schreiter et al. (2020). However, similar to the changes in the carbon elemental composition analysis, samples with lower ash content (SWP, SWP5) were impacted differently than biochars with a high initial ash content (SWP10, WSP, WSP5). While all biochars showed decreasing micropore volumes, the decrease is lower with higher initial ash content (e.g. SWP: −33%/−0.066 $cm^3\ g^{-1}$; SWP10: −21%/−0.039 $cm^3\ g^{-1}$). Enlargement of mesopores could also indicate a non-rigid carbon structure prone to structural deformation due to the high pressures applied as shown for

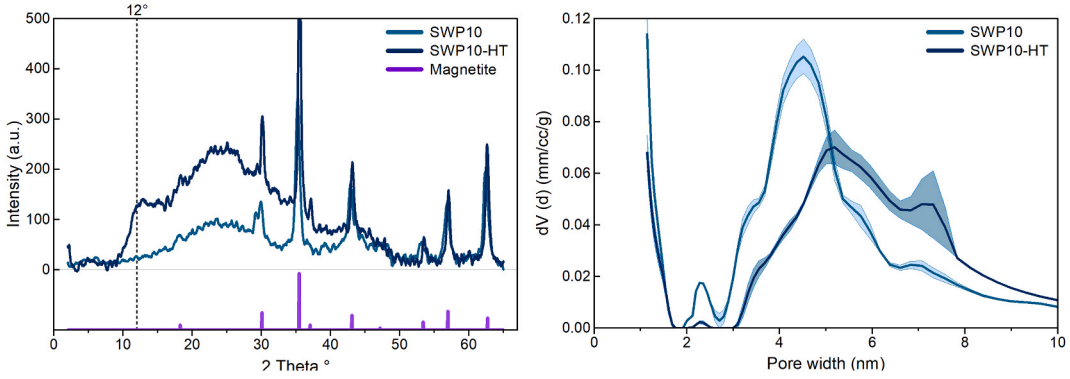

Fig. 4. Left: XRD spectra for activated softwood biochar (SWP) before and after hydrothermal treatment (HT) at 320 °C. Purple reference pattern: Magnetite - RRUFF ID: R061111.9. Right: Pore size distribution of SWP10 before and after HT at 320 °C. Mean of triplicates. Lines represent mean value of triplicate analysis; coloured area displays ±1 standard error. (For interpretation of the references to colour in this figure legend, the reader is referred to the Web version of this article.)

non-activated biochars before (Maziarka et al., 2021). Correspondingly, commercial activated carbon displayed the least structural changes after HT, which might be related to its increased carbon stability as indicated by the lowest ratio of VM to FC content of all evaluated adsorbents (Table 1). Structural rearrangements in activated biochars during HT corroborate the changes seen in the XRD spectra.

3.4. Hydrothermal recycling as an alternative treatment method

Hydrothermal treatment at 320 °C seemed to fully degrade all studied pharmaceutical parent compounds on engineered biochars and activated carbon, showing promising results as an alternative treatment method to common high-temperature thermal regeneration methods. High carbon retention (93–103%) during HT treatment is one important advantage compared to common thermal regeneration methods with typical solid mass yields between 70 and 90% and often undisclosed carbon yields (Salvador et al., 2015). Additionally, a hydrothermal treatment will provide energy benefits by using wet adsorbents, abolishing the need for heat demanding adsorbent drying prior to regeneration (Cheng et al., 2020). If used as a batch process, hydrothermal treatment might also be applied in-situ within the filter bed, potentially limiting handling losses and associated costs of transporting wet hazardous adsorbents to regeneration facilities (Gabarrell et al., 2012; Zanella et al., 2014).

As opposed to restoring the original properties of the adsorbents, the HT induced a decrease in microporosity in all biochars, while increasing the mesopore volume of the adsorbents. These structural changes might provide opportunities for subsequent uses of the treated adsorbents in different applications. A larger mesopore volume can increase the adsorption capacity for larger contaminants such as heavy metals (Hsieh and Teng, 2000; Leng et al., 2021), or enhance the nutrient adsorption capacity in an agricultural application scenario (Gong et al., 2019). In the context of a sequential biochar system, this structural alteration can be utilised to match suitable sequential uses to the changed material properties (Wurzer et al., 2019). Used as a soil amendment, recycled biochar might display beneficial properties compared to raw biochar, opening up alternative end-of-life scenarios for exhausted carbon adsorbents (Harikishore Kumar Reddy et al., 2017). Another difference in biochar properties after HT treatment compared to common thermal regeneration can be found in the preservation of oxygen-containing functional groups (Cazetta et al., 2013), which might present advantages in agricultural and environmental applications, e.g. the retention of heavy metals in soils (Uchimiya et al., 2011a).

Furthermore, a wider range of materials is suitable for hydrothermal treatment in comparison to thermal regeneration which uses oxidising gases. Here, metallic species and minerals can catalyse carbon gasification reactions and increase carbon burn-off, rendering thermal regeneration highly inefficient (Guo and Du, 2012; Lambert et al., 2002). However, inorganic impurities or purposefully introduced metallic species as found in many engineered biochars do not present disadvantages for hydrothermal recycling. The Fe-doped biochars in this study even increased the recycling efficiency under hydrothermal conditions, showcasing the potential of this method for novel carbon adsorbents.

However, there are still areas that need to be addressed to ensure the environmental safety of decontaminated biochar, such as the type, concentration, toxicity, and fate of possible transformation products of the degraded contaminants. Additionally, understanding the correlation between structural properties of the target contaminants and their required degradation temperatures would enable the identification of a minimum threshold temperature for individual contaminants. For treatment of unknown contaminant mixtures on the other hand, understanding potential synergistic and/or antagonistic effects may be required as well. For future studies, assessment of a broader set of organic pollutants, the impact of natural organic matter on the degradation performance, and the effects of incorporated catalysts on recycling of engineered biochar should be addressed to allow a more comprehensive evaluation of hydrothermal treatment as an alternative recycling method for carbon adsorbents.

4. Conclusions

Hydrothermal treatment was shown to be a viable method to degrade pharmaceuticals at temperatures of at least 320 °C. However, prior adsorption to carbon adsorbents protected two out of the 10 studied contaminants from degradation, leading to incomplete conversion of the parent compounds on non-doped activated biochar. Nonetheless, the efficiency of the hydrothermal treatment was increased by using specifically engineered biochars with Fe-doped surface functionality. We previously showed that the Fe-doped biochars display higher production efficiencies and improved adsorption capacities compared to their unamended counterparts (Wurzer and Mašek, 2021), while an increased recycling efficiency was observed within this study. These parallel benefits highlight the potential of designing biochars to increase their performance beyond a single application phase. The activated biochars were generally stable even in the harshest hydrothermal conditions used (320 °C) with a carbon retention of more than 93%, which further supports the viability of the treatment and preserves the carbon sequestration potential of biochar. Importantly, the observed HT-induced changes in biochar structural properties such as an increased mesopore volume can be beneficial for subsequent applications within a sequential biochar system. Here, hydrothermally recycled biochar might present advantages for agricultural applications to retain nutrients or heavy metals in soil. Beside these desirable effects on the biochar properties, a hydrothermal treatment can also provide operating benefits such as removing the need to dry the adsorbent prior to recycling or its suitability for treating metal-doped engineered biochars. This study highlighted for the first time the opportunities of a HT treatment for the recycling of biochar and paves the way for novel solutions in dealing with exhausted carbon adsorbents.

Credit author statement

Christian Wurzer: Conceptualization. Methodology. Formal analysis. Investigation. Resources. Writing – original draft. Visualization. **Pierre Oesterle**: Conceptualization. Methodology. Formal analysis. Investigation. Writing – review & editing. **Stina Jansson:** Conceptualization. Resources. Writing – review & editing. Supervision. Project administration. Funding acquisition. **Ondřej Mašek:** Conceptualization. Resources. Writing – review & editing. Supervision. Project administration. Funding acquisition.

Declaration of competing interest

The authors declare that they have no known competing financial interests or personal relationships that could have appeared to influence the work reported in this paper.

Data availability

Data will be made available on request.

Acknowledgements

This project received funding from the European Union's Horizon 2020 research and innovation programme under the Marie Skłodowska-Curie grant agreement No 721991. The authors also acknowledge Bio4Energy (www.bio4energy.se), a strategic research environment appointed by the Swedish government, for supporting this work. We also thank András Gorzsás at the Vibrational Spectroscopy Core Facility at Umeå University for his support.

Appendix A. Supplementary data

Supplementary data to this article can be found online at https://doi.org/10.1016/j.envpol.2022.120532.

References

Abdel-Moety, E.M., Khattab, F.I., Kelani, K.M., AbouAl-Alamein, A.M., 2002. Chromatographic determination of clotrimazole, ketoconazole and fluconazole in pharmaceutical formulations. Farmaco 57, 931–938. https://doi.org/10.1016/S0014-827X(02)01270-3.

Ahmed, M.B., Zhou, J.L., Ngo, H.H., Guo, W., 2015. Adsorptive removal of antibiotics from water and wastewater: progress and challenges. Sci. Total Environ. 532, 112–126. https://doi.org/10.1016/j.scitotenv.2015.05.130.

Akiya, N., Savage, P.E., 2002. Roles of water for chemical reactions in high-temperature water. Chem. Rev. 102, 2725–2750. https://doi.org/10.1021/cr000668w.

Alhashimi, H.A., Aktas, C.B., 2017. Life cycle environmental and economic performance of biochar compared with activated carbon: a meta-analysis. Resour. Conserv. Recycl. 118, 13–26. https://doi.org/10.1016/j.resconrec.2016.11.016.

Baresel, C., Harding, M., Fang, J., 2019. Ultrafiltration/granulated active carbon-biofilter: efficient removal of a broad range of micropollutants. Appl. Sci. 9 https://doi.org/10.3390/app9040710.

Cai, N., Larese-Casanova, P., 2014. Sorption of carbamazepine by commercial graphene oxides: a comparative study with granular activated carbon and multiwalled carbon nanotubes. J. Colloid Interface Sci. 426, 152–161. https://doi.org/10.1016/j.jcis.2014.03.038.

Cazetta, A.L., Junior, O.P., Vargas, A.M.M., Da Silva, A.P., Zou, X., Asefa, T., Almeida, V. C., 2013. Thermal regeneration study of high surface area activated carbon obtained from coconut shell: Characterization and application of response surface methodology. J. Anal. Appl. Pyrolysis 101, 53–60. https://doi.org/10.1016/j.jaap.2013.02.013.

Cheng, F., Luo, H., Colosi, L.M., 2020. Slow pyrolysis as a platform for negative emissions technology: an integration of machine learning models, life cycle assessment, and economic analysis. Energy Convers. Manag. 223, 113258 https://doi.org/10.1016/j.enconman.2020.113258.

Collard, F.X., Blin, J., Bensakhria, A., Valette, J., 2012. Influence of impregnated metal on the pyrolysis conversion of biomass constituents. J. Anal. Appl. Pyrolysis 95, 213–226. https://doi.org/10.1016/j.jaap.2012.02.009.

Dastgheib, S.A., Ren, J., Rostam-Abadi, M., Chang, R., 2014. Preparation of functionalized and metal-impregnated activated carbon by a single-step activation method. Appl. Surf. Sci. 290, 92–101. https://doi.org/10.1016/j.apsusc.2013.11.005.

De Souza, F.S., Gonçalves, R.S., Spinelli, A., 2014. Assessment of caffeine adsorption onto mild steel surface as an eco-friendly corrosion inhibitor. J. Braz. Chem. Soc. 25, 81–90. https://doi.org/10.5935/0103-5053.20130270.

Dittmann, D., Eisentraut, P., Goedecke, C., Wiesner, Y., Jekel, M., Ruhl, A.S., Braun, U., 2020. Specific adsorption sites and conditions derived by thermal decomposition of activated carbons and adsorbed carbamazepine. Sci. Rep. 10, 1–13. https://doi.org/10.1038/s41598-020-63481-y.

Duan, W., Oleszczuk, P., Pan, B., Xing, B., 2019. Environmental behavior of engineered biochars and their aging processes in soil. Biochar 1, 339–351. https://doi.org/10.1007/s42773-019-00030-5.

Duan, X.H., Srinivasa Kannan, C., Qu, W.W., Wang, X., Peng, J.H., Zhang, L.B., Xia, H.Y., 2012. Thermal regeneration of spent coal-based activated carbon using carbon dioxide: process optimisation, Methylene Blue decolorisation isotherms and kinetics. Color. Technol. 128, 464–472. https://doi.org/10.1111/j.1478-4408.2012.00401.x.

Dutta, T., Kim, T., Vellingiri, K., Tsang, D.C.W., Shon, J.R., Kim, K.H., Kumar, S., 2019. Recycling and regeneration of carbonaceous and porous materials through thermal or solvent treatment. Chem. Eng. J. 364, 514–529. https://doi.org/10.1016/j.cej.2019.01.049.

Faheem, Du, J., Kim, S.H., Hassan, M.A., Irshad, S., Bao, J., 2020. Application of biochar in advanced oxidation processes: supportive, adsorptive, and catalytic role. Environ. Sci. Pollut. Res. 27, 37286–37312. https://doi.org/10.1007/s11356-020-07612-y.

Falamarzian, S., Tavakoli, O., Zarghami, R., Faramarzi, M.A., 2014. Catalytic hydrothermal treatment of pharmaceutical wastewater using sub- and supercritical water reactions. J. Supercrit. Fluids 95, 265–272. https://doi.org/10.1016/j.supflu.2014.07.017.

Fdez-Sanromán, A., Pazos, M., Rosales, E., Sanromán, M.A., 2020. Unravelling the environmental application of biochar as low-cost biosorbent: a review. Appl. Sci. 10, 1–22. https://doi.org/10.3390/app10217810.

Frigerio, A., Baker, K.M., Belvedere, G., 1973. Gas chromatographic degradation of several drugs and their metabolites. Anal. Chem. 45, 1846–1851. https://doi.org/10.1021/ac60333a040.

Gabarrell, X., Font, M., Vicent, T., Caminal, G., Sarrà, M., Blánquez, P., 2012. A comparative life cycle assessment of two treatment technologies for the Grey Lanaset G textile dye: Biodegradation by Trametes versicolor and granular activated carbon adsorption. Int. J. Life Cycle Assess. 17, 613–624. https://doi.org/10.1007/s11367-012-0385-z.

Gong, H., Tan, Z., Zhang, L., Huang, Q., 2019. Preparation of biochar with high absorbability and its nutrient adsorption–desorption behaviour. Sci. Total Environ. 694, 133728 https://doi.org/10.1016/j.scitotenv.2019.133728.

Guo, Y., Du, E., 2012. The effects of thermal regeneration conditions and inorganic compounds on the characteristics of activated carbon used in power plant. Energy Proc. 17, 444–449. https://doi.org/10.1016/j.egypro.2012.02.118.

Hagemann, N., Spokas, K., Schmidt, H.P., Kägi, R., Böhler, M.A., Bucheli, T.D., 2018. Activated carbon, biochar and charcoal: Linkages and synergies across pyrogenic carbon's ABCs. Water (Switzerland) 10, 1–19. https://doi.org/10.3390/w10020182.

Harikishore Kumar Reddy, D., Vijayaraghavan, K., Kim, J.A., Yun, Y.S., 2017. Valorisation of post-sorption materials: opportunities, strategies, and challenges. Adv. Colloid Interface Sci. 242, 35–58. https://doi.org/10.1016/j.cis.2016.12.002.

Hsieh, C.T., Teng, H., 2000. Influence of mesopore volume and adsorbate size on adsorption capacities of activated carbons in aqueous solutions. Carbon N. Y. 38, 863–869. https://doi.org/10.1016/S0008-6223(99)00180-3.

Huang, H.J., Yuan, X.Z., 2016. The migration and transformation behaviors of heavy metals during the hydrothermal treatment of sewage sludge. Bioresour. Technol. 200, 991–998. https://doi.org/10.1016/j.biortech.2015.10.099.

Jang, H.M., Kan, E., 2019. Engineered biochar from agricultural waste for removal of tetracycline in water. Bioresour. Technol. 284, 437–447. https://doi.org/10.1016/j.biortech.2019.03.131.

Joseph, B., Kaetzl, K., Hensgen, F., Schäfer, B., Wachendorf, M., 2020. Sustainability assessment of activated carbon from residual biomass used for micropollutant removal at a full-scale wastewater treatment plant. Environ. Res. Lett. 15 https://doi.org/10.1088/1748-9326/ab8330.

Jung, S.H., Kim, J.S., 2014. Production of biochars by intermediate pyrolysis and activated carbons from oak by three activation methods using CO2. J. Anal. Appl. Pyrolysis 107, 116–122. https://doi.org/10.1016/j.jaap.2014.02.011.

Kårelid, V., Larsson, G., Björlenius, B., 2017. Pilot-scale removal of pharmaceuticals in municipal wastewater: comparison of granular and powdered activated carbon treatment at three wastewater treatment plants. J. Environ. Manag. 193, 491–502. https://doi.org/10.1016/j.jenvman.2017.02.042.

Kozyatnyk, I., Yacout, D.M.M., Van Caneghem, J., Jansson, S., 2020. Comparative environmental assessment of end-of-life carbonaceous water treatment adsorbents. Bioresour. Technol. 302, 122866 https://doi.org/10.1016/j.biortech.2020.122866.

Krasucka, P., Pan, B., Sik Ok, Y., Mohan, D., Sarkar, B., Oleszczuk, P., 2021. Engineered biochar – a sustainable solution for the removal of antibiotics from water. Chem. Eng. J. 405, 126926 https://doi.org/10.1016/j.cej.2020.126926.

Lambert, S.D., San Miguel, G., Graham, N.J.D., 2002. Deleterious effects of inorganic compounds during thermal regeneration of GAC: a review. J. Am. Water Works Assoc. 94, 109–119. https://doi.org/10.1002/j.1551-8833.2002.tb10253.x.

Leng, L., Xiong, Q., Yang, L., Li, Hui, Zhou, Y., Zhang, W., Jiang, S., Li, Hailong, Huang, H., 2021. An overview on engineering the surface area and porosity of biochar. Sci. Total Environ. 763 https://doi.org/10.1016/j.scitotenv.2020.144204.

Lindberg, R.H., Östman, M., Olofsson, U., Grabic, R., Fick, J., 2014. Occurrence and behaviour of 105 active pharmaceutical ingredients in sewage waters of a municipal sewer collection system. Water Res. 58, 221–229. https://doi.org/10.1016/j.watres.2014.03.076.

Liu, Y., He, Z., Uchimiya, M., 2015. Comparison of biochar formation from various agricultural by-products sing FTIR spectroscopy. Mod. Appl. Sci. 9, 246–253. https://doi.org/10.5539/mas.v9n4p246.

Liyanage, A.S., Canaday, S., Pittman, C.U., Mlsna, T., 2020. Rapid remediation of pharmaceuticals from wastewater using magnetic Fe3O4/Douglas fir biochar adsorbents. Chemosphere 258, 127336. https://doi.org/10.1016/j.chemosphere.2020.127336.

Loos, Robert, Carvalho, Raquel, Antonio, Diana, Comero, Sara, Locoro, Giovanni, Tavazzi, Simona, Paracchini, Bruno, Ghiani, Michela, Lettieri, Teresa, Blaha, Ludek, Jarosova, Barbora, Voorspoels, Stefan, Servaes, Kelly, Haglund, Peter, Fick, Jerker, Lindberg, Richard, Schwesig, David, Gawlik, Bernd, 2013. EU-wide monitoring survey on emerging polar organic contaminants in wastewater treatment plant effluents. Water Res. 47, 6475–6487. https://doi.org/10.1016/j.watres/2013.08.024.

Lou, K., Rajapaksha, A.U., Ok, Y.S., Chang, S.X., 2016. Pyrolysis temperature and steam activation effects on sorption of phosphate on pine sawdust biochars in aqueous solutions. Chem. Speciat. Bioavailab. 28, 42–50. https://doi.org/10.1080/09542299.2016.1165080.

Lyu, H., Tang, J., Cui, M., Gao, B., Shen, B., 2020. Biochar/iron (BC/Fe) composites for soil and groundwater remediation: synthesis, applications, and mechanisms. Chemosphere 246, 125609. https://doi.org/10.1016/j.chemosphere.2019.125609.

Ma, F., Zhao, B., Diao, J., Jiang, Y., Zhang, J., 2020. Mechanism of phosphate removal from aqueous solutions by biochar supported nanoscale zero-valent iron. RSC Adv. 10, 39217–39225. https://doi.org/10.1039/d0ra07391a.

Maziarka, P., Wurzer, C., Arauzo, P.J., Dieguez-Alonso, A., Mašek, O., Ronsse, F., 2021. Do you BET on routine? The reliability of N2 physisorption for the quantitative assessment of biochar's surface area. Chem. Eng. J. 418 https://doi.org/10.1016/j.cej.2021.129234.

Mustafa, M., Kozyatnyk, I., Gallampois, C., Oesterle, P., Östman, M., Tysklind, M., 2021. Regeneration of saturated activated carbon by electro-peroxone and ozonation: fate of micropollutants and their transformation products. Sci. Total Environ. 776, 145723 https://doi.org/10.1016/j.scitotenv.2021.145723.

Nguyen, V.T., Nguyen, T.B., Chen, C.W., Hung, C.M., Huang, C.P., Dong, C. Di, 2019. Cobalt-impregnated biochar (Co-SCG) for heterogeneous activation of peroxymonosulfate for removal of tetracycline in water. Bioresour. Technol. 292, 121954 https://doi.org/10.1016/j.biortech.2019.121954.

Oesterle, P., Lindberg, R.H., Fick, J., Jansson, S., 2020. Extraction of active pharmaceutical ingredients from simulated spent activated carbonaceous adsorbents. Environ. Sci. Pollut. Res. 27, 25572–25581. https://doi.org/10.1007/s11356-020-08822-0.

OSPAR Commission, 2005. Hazardous Substances Series - Clotrimazole.

Patel, M., Kumar, R., Kishor, K., Mlsna, T., Pittman, C.U., Mohan, D., 2019. Pharmaceuticals of emerging concern in aquatic systems: Chemistry, occurrence,

effects, and removal methods. Chem. Rev. 119, 3510–3673. https://doi.org/10.1021/acs.chemrev.8b00299.
Pham, M., Schideman, L., Sharma, B.K., Zhang, Y., Chen, W.T., 2013. Effects of hydrothermal liquefaction on the fate of bioactive contaminants in manure and algal feedstocks. Bioresour. Technol. 149, 126–135. https://doi.org/10.1016/j.biortech.2013.08.131.
Rizzo, L., Malato, S., Antakyali, D., Beretsou, V.G., Đolić, M.B., Gernjak, W., Heath, E., Ivancev-Tumbas, I., Karaolia, P., Lado Ribeiro, A.R., Mascolo, G., McArdell, C.S., Schaar, H., Silva, A.M.T., Fatta-Kassinos, D., 2019. Consolidated vs new advanced treatment methods for the removal of contaminants of emerging concern from urban wastewater. Sci. Total Environ. 655, 986–1008. https://doi.org/10.1016/j.scitotenv.2018.11.265.
Rocha, L.S., Pereira, D., Sousa, É., Otero, M., Esteves, V.I., Calisto, V., 2020. Recent advances on the development and application of magnetic activated carbon and char for the removal of pharmaceutical compounds from waters: a review. Sci. Total Environ. 718 https://doi.org/10.1016/j.scitotenv.2020.137272.
Rout, P.R., Zhang, T.C., Bhunia, P., Surampalli, R.Y., 2021. Treatment technologies for emerging contaminants in wastewater treatment plants: a review. Sci. Total Environ. 753, 141990 https://doi.org/10.1016/j.scitotenv.2020.141990.
Saadattalab, V., Wang, X., Szego, A.E., Hedin, N., 2020. Effects of metal ions, metal, and metal oxide particles on the synthesis of hydrochars. ACS Omega 5, 5601–5607. https://doi.org/10.1021/acsomega.9b03926.
Salvador, F., Jiménez, C.S., 1996. A new method for regenerating activated carbon by thermal desorption with liquid water under subcritical conditions. Carbon N. Y. 34, 511–516. https://doi.org/10.1016/0008-6223(95)00211-1.
Salvador, F., Martin-Sanchez, N., Sanchez-Montero, M.J., Montero, J., Izquierdo, C., 2013. Regeneration of activated carbons contaminated by phenol using supercritical water. J. Supercrit. Fluids 74, 1–7. https://doi.org/10.1016/j.supflu.2012.11.025.
Salvador, F., Sanchez-Montero, M.J., Izquierdo, C., Martin-Sanchez, N., Sanchez-Hernandez, R., Sanchez-Montero, M.J., Izquierdo, C., Martin-Sanchez, N., Sanchez-Hernandez, R., Sanchez-Montero, M.J., Izquierdo, C., 2015. Regeneration of carbonaceous adsorbents. Part I: thermal regeneration. Microporous Mesoporous Mater. 202, 259–276. https://doi.org/10.1016/j.micromeso.2014.02.045.
Sato, T., Takahata, T., Honma, T., Watanabe, M., Wagatsuma, M., Matsuda, S., Smith, R. L., Itoh, N., 2018. Hydrothermal extraction of antioxidant compounds from green coffee beans and decomposition kinetics of 3- o-caffeoylquinic acid. Ind. Eng. Chem. Res. 57, 7624–7632. https://doi.org/10.1021/acs.iecr.8b00821.
Schreiter, I.J., Schmidt, W., Kumar, A., Graber, E.R., Schüth, C., 2020. Effect of water leaching on biochar properties and its impact on organic contaminant sorption. Environ. Sci. Pollut. Res. 27, 691–703. https://doi.org/10.1007/s11356-019-06904-2.
Sewu, D.D., Tran, H.N., Ohemeng-Boahen, G., Woo, S.H., 2020. Facile magnetic biochar production route with new goethite nanoparticle precursor. Sci. Total Environ. 717, 137091 https://doi.org/10.1016/j.scitotenv.2020.137091.
Silva Thomsen, L.B., Carvalho, P.N., dos Passos, J.S., Anastasakis, K., Bester, K., Biller, P., 2020. Hydrothermal liquefaction of sewage sludge; energy considerations and fate of micropollutants during pilot scale processing. Water Res. 183, 116101 https://doi.org/10.1016/j.watres.2020.116101.
Sizmur, T., Fresno, T., Akgül, G., Frost, H., Moreno-Jiménez, E., 2017. Biochar modification to enhance sorption of inorganics from water. Bioresour. Technol. https://doi.org/10.1016/j.biortech.2017.07.082.
Smith, A.M., Singh, S., Ross, A.B., 2016. Fate of inorganic material during hydrothermal carbonisation of biomass: influence of feedstock on combustion behaviour of hydrochar. Fuel 169, 135–145. https://doi.org/10.1016/j.fuel.2015.12.006.
Sühnholz, S., Kopinke, F.D., Weiner, B., 2018. Hydrothermal treatment for regeneration of activated carbon loaded with organic micropollutants. Sci. Total Environ. 644, 854–861. https://doi.org/10.1016/j.scitotenv.2018.06.395.
Sun, P., Heng, M., Sun, S., Chen, J., 2010. Direct liquefaction of paulownia in hot compressed water: influence of catalysts. Energy 35, 5421–5429. https://doi.org/10.1016/j.energy.2010.07.005.
Svahn, O., Björklund, E., 2015. Thermal stability assessment of antibiotics in moderate temperature and subcriticalwater using a pressurized dynamic flow-through system. Int. J. Innovat. Appl. Stud. 11, 872–880.
Taboada-Santos, A., Braz, G.H.R., Fernandez-Gonzalez, N., Carballa, M., Lema, J.M., 2019. Thermal hydrolysis of sewage sludge partially removes organic micropollutants but does not enhance their anaerobic biotransformation. Sci. Total Environ. 690, 534–542. https://doi.org/10.1016/j.scitotenv.2019.06.492.
Thakur, S., Kumar, A., Reddy, S.N., 2019. Hydrothermal treatment of pharmaceutical wastewater. Indian Chem. Eng. 61, 415–423. https://doi.org/10.1080/00194506.2019.1608869.
Thompson, K.A., Shimabuku, K.K., Kearns, J.P., Knappe, D.R.U., Summers, R.S., Cook, S. M., 2016. Environmental comparison of biochar and activated carbon for tertiary wastewater treatment. Environ. Sci. Technol. 50, 11253–11262. https://doi.org/10.1021/acs.est.6b03239.
Uchimiya, M., Chang, S.C., Klasson, K.T., 2011a. Screening biochars for heavy metal retention in soil: role of oxygen functional groups. J. Hazard Mater. 190, 432–441. https://doi.org/10.1016/j.jhazmat.2011.03.063.
Uchimiya, M., Wartelle, L.H., Klasson, K.T., Fortier, C.A., Lima, I.M., 2011b. Influence of pyrolysis temperature on biochar property and function as a heavy metal sorbent in soil. J. Agric. Food Chem. 59, 2501–2510. https://doi.org/10.1021/jf104206c.
vom Eyser, C., Palmu, K., Schmidt, T.C., Tuerk, J., 2015. Pharmaceutical load in sewage sludge and biochar produced by hydrothermal carbonization. Sci. Total Environ. 537, 180–186. https://doi.org/10.1016/j.scitotenv.2015.08.021.
Wang, L., Ok, Y.S., Tsang, D.C.W., Alessi, D.S., Rinklebe, J., Wang, H., Mašek, O., Hou, R., O'Connor, D., Hou, D., 2020. New trends in biochar pyrolysis and modification strategies: feedstock, pyrolysis conditions, sustainability concerns and implications for soil amendment. Soil Use Manag. 36, 358–386. https://doi.org/10.1111/sum.12592.
Weiner, B., Baskyr, I., Poerschmann, J., Kopinke, F.D., 2013. Potential of the hydrothermal carbonization process for the degradation of organic pollutants. Chemosphere 92, 674–680. https://doi.org/10.1016/j.chemosphere.2013.03.047.
Weiner, B., Suhnholz, S., Kopinke, F.D., 2017. Hydrothermal conversion of triclosan-the role of activated carbon as sorbent and reactant. Environ. Sci. Technol. 51, 1649–1653. https://doi.org/10.1021/acs.est.6b05314.
Wurzer, C., Mašek, O., 2021. Feedstock doping using iron rich waste increases the pyrolysis gas yield and adsorption performance of magnetic biochar for emerging contaminants. Bioresour. Technol. 321 https://doi.org/10.1016/j.biortech.2020.124473.
Wurzer, C., Sohi, S., Masek, O., 2019. Synergies in sequential biochar systems. In: Manyà, J.J. (Ed.), Advanced Carbon Materials from Biomass - an Overview, pp. 147–159. https://doi.org/10.5281/ZENODO.3233733. Zenodo.
Xia, S., Li, K., Xiao, H., Cai, N., Dong, Z., xu, C., Chen, Y., Yang, H., Tu, X., Chen, H., 2019. Pyrolysis of Chinese chestnut shells: effects of temperature and Fe presence on product composition. Bioresour. Technol. 287 https://doi.org/10.1016/j.biortech.2019.121444.
Yi, Y., Huang, Z., Lu, B., Xian, J., Tsang, E.P., Cheng, W., Fang, J., Fang, Z., 2019. Magnetic biochar for environmental remediation: a review. Bioresour. Technol. 298 https://doi.org/10.1016/j.biortech.2019.122468.
Zanella, O., Tessaro, I.C., Féris, L.A., 2014. Desorption- and decomposition-based techniques for the regeneration of activated carbon. Chem. Eng. Technol. 37, 1447–1459. https://doi.org/10.1002/ceat.201300808.